Electronic Supplementary Material (ESI) for Physical Chemistry Chemical Physics.

Supporting Information

A new planar BCN lateral heterostructure with outstanding strength and defect-mediated superior semiconducting to conducting properties

Siby Thomas and Mohsen Asle Zaeem*

Department of Mechanical Engineering, Colorado School of Mines, 1500 Illinois St., Golden, Colorado - 80401, USA.

*Corresponding author. E-mail: zaeem@mines.edu (M. Asle Zaeem)

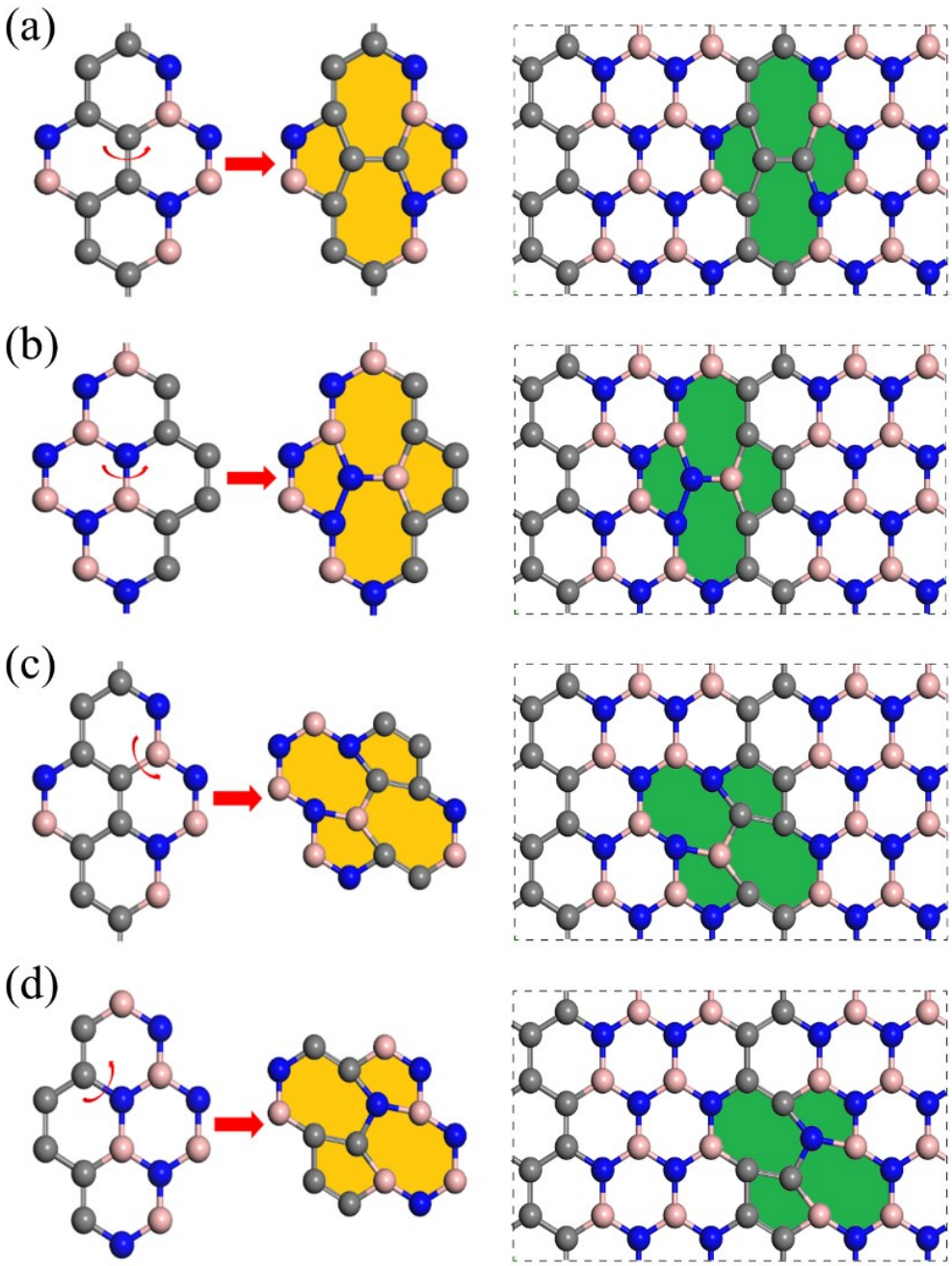

Fig. S1 Schematic of the formation of Stone-Wales defects in the BCN heterostructure such as (a) SW-$CC_{AC,}$ (b) SW-$BN_{AC,}$ (c) SW-BC_{ZZ} and (d) SW-$CN_{ZZ.}$ A Stone-Wales defect is a topological defect formed by changing the connectivity of a pair of 6- membered rings by a rotation of 90º, leading to the formation of two 5- membered and two 7- membered rings, as shown in the figure.

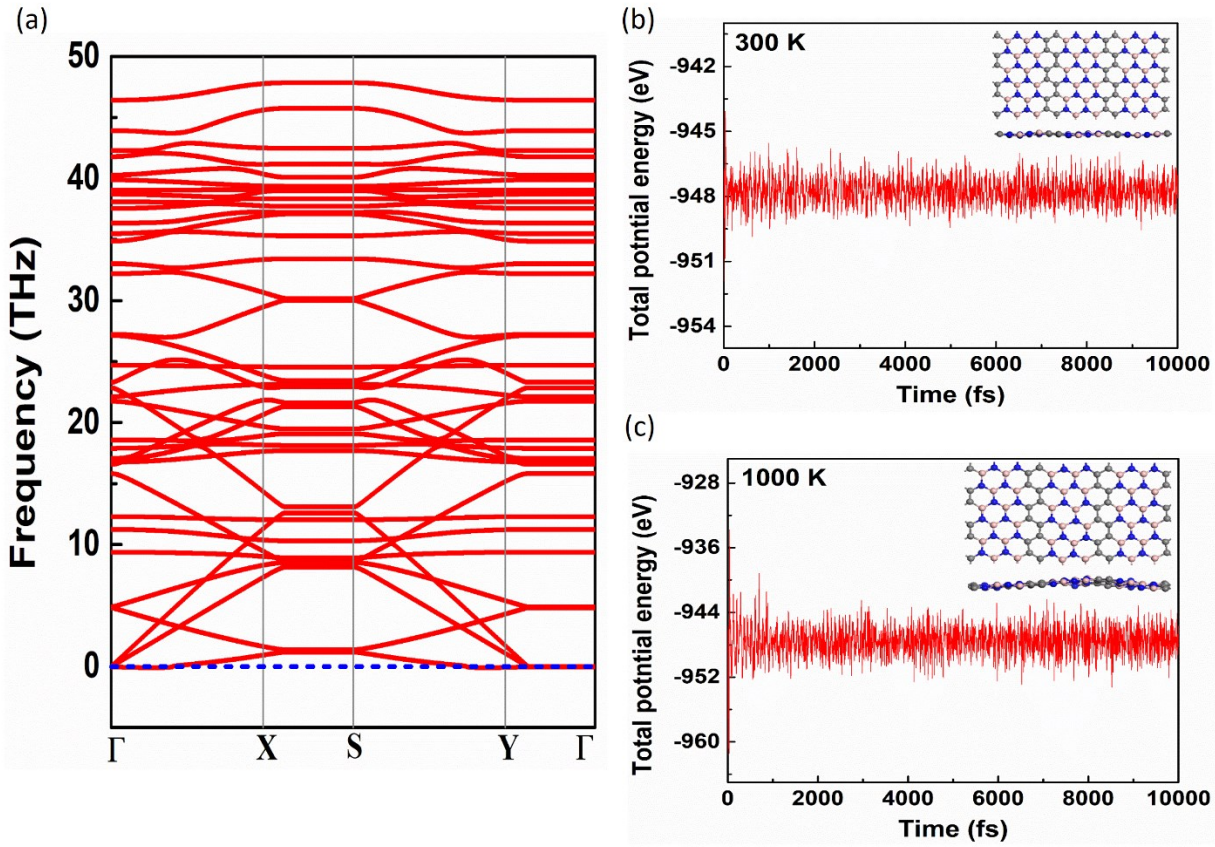

Fig. S2 (a) Phonon dispersion spectra of BCN heterostructure computed using the supercell approach. The positive phonon modes throughout the Brillouin zone confirms the dynamical stability of the structure. Fluctuation of the total potential energy during the AIMD simulation at (b) 300 K and (c)1000 K with a supercell of 3×3. Insets are snapshots of the structure at the end of the simulation.

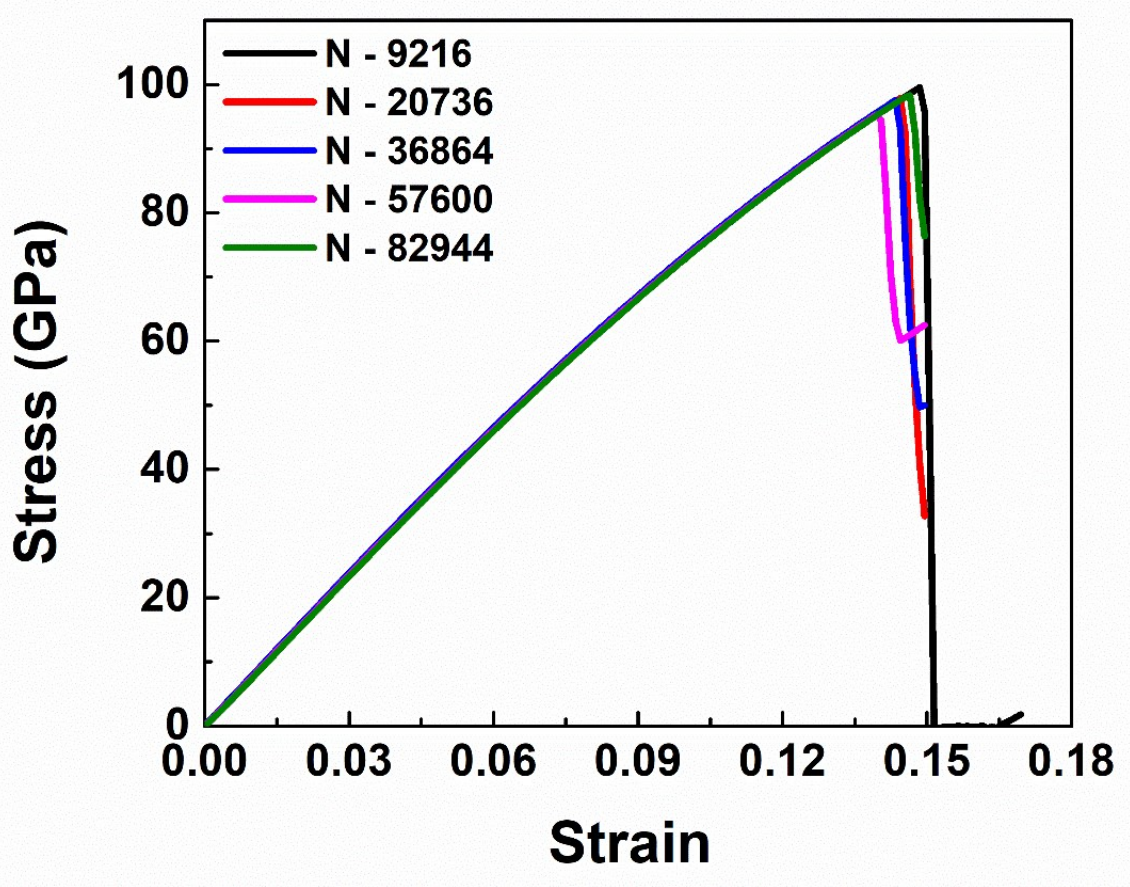

Fig. S3 The size dependence in the stress-strain response of pristine BCN heterostructure at 300 K using different system size (N) consist of 9216, 20,736, 36,864, 57,600, and 82,944 atoms.

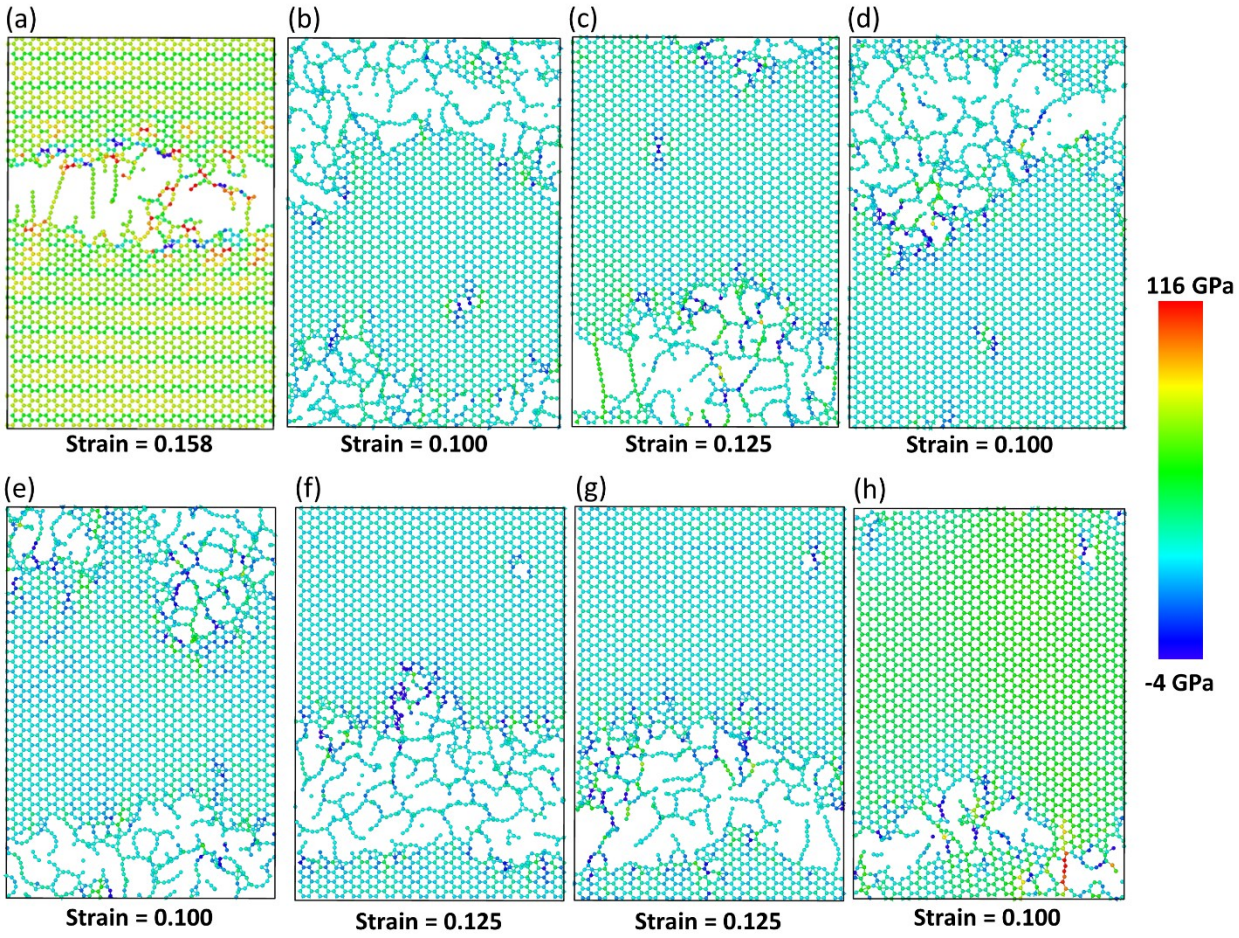

Fig. S4 Illustration of the stress distributions over the atoms in (a) pristine, (b) - (e) Stone-Wales defect filled, and (f) - (g) vacancy filled BCN heterostructure with 0.1% defect concentration at the time of failure along the armchair direction at 300 K.

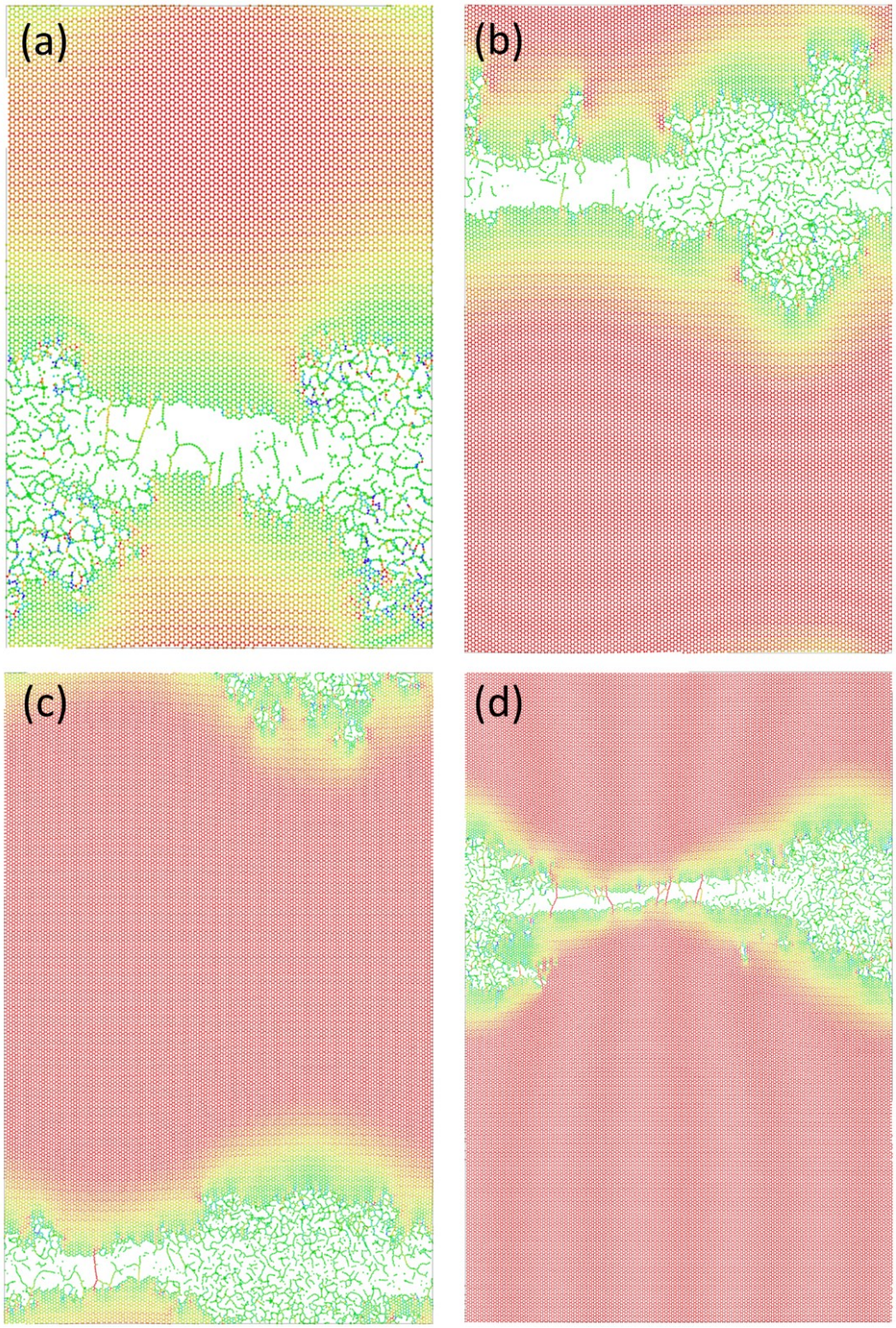

Fig. S5 Illustration of the failure morphology of pristine BCN heterostructure at 300 K using different system size consist of (a) 20,736, (b) 36,864, (c) 57,600, and (d) 82,944 atoms.

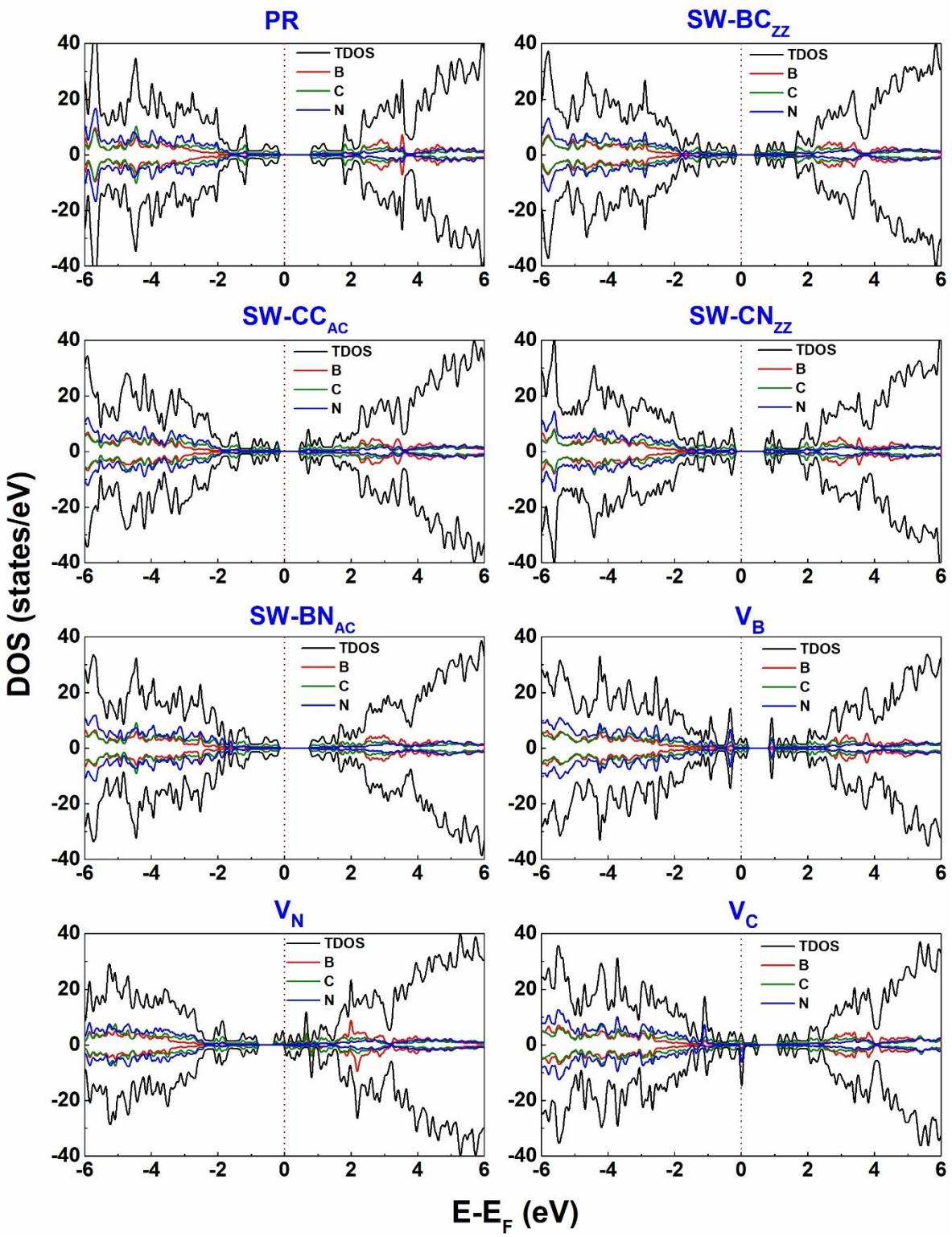

Fig. S6 Total and partial electronic density of states of pristine BCN, SW-BC_{ZZ}, SW-$CC_{AC,}$ SW-CNZZ, SW-BN_{AC}, V_B, V_N, and V_C. The contributions from B, C, and N atoms are also provided. The vertical wine colored dashed line indicates the Fermi level.

Table S1. Mechanical properties of the pristine and defective BCN heterostructures calculated along the zigzag (ZZ or E_x) and armchair (AC or E_y) directions. Here, AC and ZZ in the subscript of the SW defect denote the respective bond orientation for the creation of a SW defect along with the armchair and zigzag orientations. The V_B, V_N, and V_C represent the single atom vacancy of B, N and C, respectively. For comparison, the corresponding values of graphene, h-BN and another BCN structure are also provided.

	Elastic Constant (N/m)				Young's modulus (N/m)		Poisson's ratio	
	C_{11}	C_{22}	C_{12}	C_{66}	E_x	E_y	ν_x	ν_y
Pristine	305.68	307.72	64.71	122.00	291.98	294.11	0.21	0.21
SW-BC_{ZZ}	295.38	292.48	64.86	116.76	281.14	278.09	0.22	0.22
SW-CC_{AC}	293.14	298.85	64.36	115.17	279.01	284.99	0.22	0.22
SW-CN_{ZZ}	297.15	293.63	66.70	116.07	282.18	278.48	0.22	0.23
SW-BN_{AC}	286.80	295.99	63.94	113.34	272.55	282.18	0.22	0.22
V_B	217.40	254.35	80.03	106.71	187.94	229.17	0.37	0.31
V_N	258.39	272.00	56.59	102.78	246.00	260.23	0.22	0.21
V_C	271.46	283.85	64.02	112.34	256.37	269.41	0.24	0.23
Graphene[1,2]	361.70	362.72	66.47	147.59	349.48	350.53	0.18	0.18
h-BN[3]	274.71	282.50	66.10	96.44	258.80	282.03	0.24	0.23
BCN[4,5]	289.70	300.51	60.06	122.64	277.25	288.50	0.21	0.20

References

1. S. Thomas, H. Jung, S. Kim, B. Jun, C. H. Lee and S. U. Lee. *Carbon*, 2019, **148**, 344–353.
2. S. Thomas, K. M. Ajith, S. U. Lee and M. C. Valsakumar. *RSC Adv.*, 2018, **8**, 27283–27292.
3. S. Thomas, K. M. Ajith and M. C. Valsakumar. *J. Phys. Condens. Matter*, 2016, **28**, 295302.

4. S. Thomas and S. U. Lee. *RSC Adv.*, 2019, **9**, 1238–1246.

5. S. Thomas, M. S. Manju, K. M. Ajith, S. U. Lee and M. Asle Zaeem. *Phys. E Low-Dimens. Syst. Nanostructures*, 2020, **123**, 114180.